

JITTER STUDY FOR THE APS LINAC PHOTO-INJECTOR BEAM*

D. Hui^{1,†}, Y. Sun, M. Borland, J. Byrd

Advanced Photon Source, Argonne National Laboratory, Argonne, Chicago, USA

¹also at Chinese Academy of Sciences, Beijing, China

Abstract

The APS Linac photo-injector can deliver high brightness electron beams to the Linac Extension Area (LEA) for beam experiments such as TESSA (Tapering Enhanced Stimulated Superradiant Amplification). Beam jitter in the device-under-test (DUT) area of the LEA can adversely affect the quality of data for such experiments. In this paper, a start-to-end simulation of jitter is studied. Sources of jitter include photo-cathode drive-laser arrival time, laser energy, and RF phases and voltages of the photo-cathode gun and accelerating cavities. It is found that at the DUT the relative mean energy jitter is the most significant concern, and that improvements in the Linac RF voltage stability can help to reduce it. RMS energy spread are more sensitive to the laser timing and charge jitter. The laser timing jitter itself can be compressed by the magnetic chicane by a factor of 5.6.

INTRODUCTION

The APS LEA, which is downstream of the APS injector Linac, is designed and being built at Argonne National Laboratory (ANL) to provide high brightness electron beams for advanced beam experiments such as Tapering Enhanced Stimulated Superradiant Amplification (TESSA) and dielectric wakefield accelerator [1-3]. The photo-injector, which is equipped with an upgraded LCLS style Photo-Cathode Gun (PCG), will deliver the high brightness electron beams through the injector Linac down to the LEA.

The high brightness beam in the LEA experiment chamber is dedicated to small aperture apparatuses. Beam jitters in the device-under-test (DUT) area of LEA result in the degradation of the beam quality (such as emittance and energy spread growth, bunch arrival time and bunch length jitters), which will adversely affect the quality of data for the experiments. Characterization of the beam jitter and knowledge about its possible origins are of great importance to compensate or reduce the jitters for future stability improvements of the system. In this paper, *Astra* [4] and *Elegant* [5] codes are combined to study the beam jitter and sensitivity to various jitter sources including photo-cathode drive-laser arrival time and energy (i.e. charge), gun and Linac RF phases and voltages. Beam parameters of particular interest are the relative mean energy, energy spread, bunch arrival time, bunch length etc. Firstly, the beam responses at the DUT to each jitter source are studied, and then the combined effects with jitter in all sources. Jitter correlations between all the

studied jitter sources and key beam properties at the DUT are also studied.

APS LINAC AND LEA OVERVIEW

Figure 1 shows a schematic of the APS Linac down to LEA. There are two thermionic RF guns, RG1 and RG2, for usual injector operation (RG1 is a back-up). The PCG, with a maximum field gradient of 120 MV/m, is at the front end of the Linac. And a 3m S-band accelerating structure- "L1", is equipped downstream of it, delivering the PCG beam to an energy of approximately 40-45 MeV. Then three accelerating sectors known as Linac Two, Linac Four, and Linac Five ("L2", "L4" and "L5") is followed. Each sector uses a single SLEDded klystron to drive four S-band accelerating structures, accelerating the beam to a total energy up to 375-500 MeV at the end of L5. A bunch compressor chicane (R56=-65) is set behind the L2 to realize the bunch length compression with a given energy chirp [6], so that provide higher bunch brightness beam into the LEA experiment area. Three fast switching dipole magnets are set downstream of the Linac structure to ensure the interleaving operation for RG beam and PCG beam. During the RG beam operation, the three fast switching dipole magnets are turned on to inject the beam into and extract out of the PAR, and then send into the Booster. These magnets are all turned off during the PCG beam operation, so that the PCG beam will bypass the PAR and Booster, then go straight to the LEA [7]. The RG beam for APS storage ring and the PCG beam for LEA will be operated simultaneously though the Linac in an interleaved fashion. The experiment area in the LEA tunnel is where the DUT will be installed. It is sufficient to accommodate DUTs with up to 2m length. To measure the effect of the DUT on the electron beam, a magnetic spectrometer and several diagnostic YAG screens (not shown here) are also installed downstream of the DUT.

START-TO-END JITTER STUDY

In order to understand the beam properties in the DUT under various jitter sources and provide a guidance for the jitter tolerances of the global Linac, an elaborate beam jitter study using tracking codes has been performed. The simulations apply repeated 6D particle tracking for 150 times with 10k macro-particles per tracked beam pulse while varying machine parameters such as photo-cathode drive-laser arrival time and energy, gun and Linac RF phases and voltages. Also, a beam file with no errors is used as an ideal reference case. The reference bunch is

*Work supported by the U.S. Department of Energy, Office of Science, under Contract No. DE-AC02-06CH11357.

† dhui@anl.gov

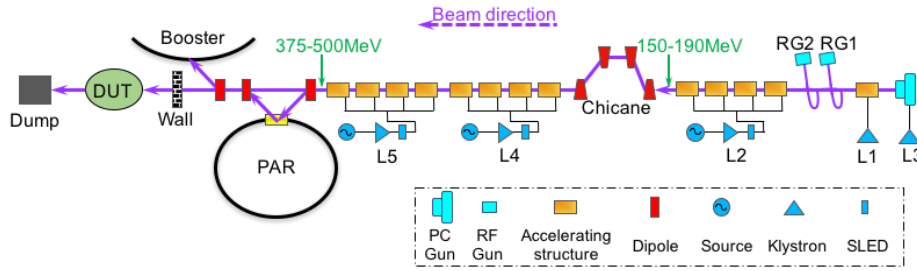


Figure 1: Schematic of the APS Linac down to LEA. Linac rf systems L2, L4, and L5 have a common source, klystron, and SLED configuration.

taken to establish the reference phases and momentum profile. The nominal beam parameters in the simulation are shown in Table 1. In the jitter simulation, *Astra* is employed to simulate the photoinjector (from photocathode to the end of L1) with the space charge and Schottky effect taken into consideration. And the *Elegant* is used for the remainder of the Linac and the LEA beamline. The output particle distributions in 6D phase space of 150 seeds from *Astra* are generated and converted into the *Elegant* input format. In the *Elegant* simulation, longitudinal and transverse wakefields of the accelerating structure, coherent synchrotron radiation (CSR) in the dipoles are included.

The jitters are generated using Gaussian distribution with a $\pm 3\sigma$ cut-off. Its RMS levels have been considered according to the realistic situation, as shown in first two columns of Table 2. The RMS error of laser timing is assumed to be 0.9 ps, about 1 degree for the 2856 MHz RF of the photo-cathode. The RMS fluctuations in charge per bunch is 5%, corresponding to the laser energy jitter of 5%. All the RF cavities, i.e. the photo-cathode gun and accelerating structure, are taken to have jitter in phase of 0.5 degrees and jitter in peak voltage of 0.5%. The jitters of separate elements are assumed to not have any correlations between different sections. However, the laser timing error will lead to a phase offset not only for the PCG, but with all subsequent accelerator structures, which will have a strong correlation through the entire beamline. The charge fluctuation will also propagate through the beam line via the wakefields in the accelerator structures and the space charge effect when the beam is at low energy level.

Table 1: Nominal Beam Parameters in the Simulation

Parameter	Value	Unit
Bunch charge	0.3	nC
Bunch length	3	ps
Transverse spot size(rms)	0.15	mm
Initial kinetic energy	0.6	eV

Beam Jitter Response at the LEA DUT

The results of start-to-end jitter simulations with 151 random seeds (the reference beam file with nominal parameters is included) using *Astra* and *Elegant* are summarized in Table 2. Jitters of key beam parameters including relative mean energy, bunch arrival time, energy spread

and bunch length at the LEA DUT are listed. The relative mean energy and bunch arrival time for which statistics shown are averaged over the 10k macro-particles. The energy spread and bunch length are given with RMS spread over the 10k macro-particles. For the jitters response, Table 2 lists mean values and RMS deviations over the 151 simulated pulses. Where meaningful, the RMS deviations are expressed as percentages of the corresponding mean values except for the relative energy and bunch arrival time, of which the mean values are 0 so that only the RMS deviations are shown.

All the beam jitter responses change linearly with each jitter source. From each column of Table 2, we can compare which source is more responsible for each beam jitter. The most significant jitter is highlighted in yellow, and the second significant in light gold. For the relative mean energy, we can see that jitters are dominated by the fluctuations in the laser timing and all the Linac RF voltages. For the bunch arrival time jitter, the accelerating structures right before chicane, i.e. the L2 phase and voltage jitters are more responsible. L2 phase jitter of 0.5 degree induces 0.364 ps arrival time jitter, and L2 voltage jitter of 0.5% corresponds to an arrival time jitter of 0.739 ps, which will adversely affect the experiment in the DUT. Note here that the error in laser timing is compressed by the magnetic chicane, so that a 0.9 ps initial timing jitter yields a timing jitter in the compressed bunch of only 160 fs. For the RMS energy spread and bunch length jitter, the laser timing contributes the most. But luckily, the RMS energy spread jitter is of the order of 10^{-4} level, and the bunch length jitter is less than 200 fs for the given input jitters. Beam sizes and centroids are all in micro-meter level, and their normalized jitters are mostly at the order of 10^{-3} to 10^{-5} . So, jitters in beam size and centroids are not a problem, which are not shown in Table 2.

Overall, seen in column-by-column, we can find that the most serious beam jitters for the experiments in the DUT are the mean energy and bunch arrival time jitter. Considering the effect on the overall beam parameters of each jitter source (observe values row-by-row), one can conclude that jitters in the laser timing, the phase and voltage of the accelerating structures right before chicane are the main contributors to the key beam jitters at the DUT. The beam fluctuations due to the gun, L1, and the accelerating structures after chicane (i.e. L4 and L5) are much smaller.

Table 2: Response of Key Beam Parameters at the LEA DUT to the Input Jitters

Quantity	RMS jitter level	Relative mean energy	Bunch arrival time	RMS energy spread		RMS bunch length	
		RMS	RMS/ps	mean	RMS/%	mean/ps	RMS/%
laser timing	0.9ps	1.42×10^{-3}	0.162	6.33×10^{-3}	8.24	1.12	17.76
charge	5.0%	1.61×10^{-4}	0.070	6.04×10^{-3}	3.85	1.20	5.08
gun phase	0.5 deg	2.25×10^{-5}	0.007	6.08×10^{-3}	0.15	1.21	0.18
gun voltage	0.5%	7.78×10^{-5}	0.054	6.08×10^{-3}	0.08	1.22	2.48
L1 phase	0.5 deg	1.10×10^{-5}	0.003	6.07×10^{-3}	1.02	1.21	2.40
L1 voltage	0.5%	4.08×10^{-4}	0.231	6.07×10^{-3}	0.62	1.21	0.39
L2 phase	0.5 deg	6.88×10^{-4}	0.364	6.10×10^{-3}	2.51	1.20	7.47
L2 voltage	0.5%	1.37×10^{-3}	0.739	6.06×10^{-3}	2.22	1.21	0.95
L4 phase	0.5 deg	1.83×10^{-5}	0.000	6.07×10^{-3}	0.56	1.21	0.00
L4 voltage	0.5%	1.45×10^{-3}	0.001	6.07×10^{-3}	0.00	1.21	0.04
L5 phase	0.5 deg	1.83×10^{-5}	0.000	6.07×10^{-3}	0.56	1.21	0.00
L5 voltage	0.5%	1.45×10^{-3}	0.000	6.07×10^{-3}	0.00	1.21	0.04
All	---	3.07×10^{-3}	0.986	6.39×10^{-3}	11.17	1.12	20.93

Beam Jitter Development along the Beamline

In order to see the beam jitter development along the whole beamline with various input jitters, the RMS deviations of some key beam parameters over the 151 simulated pulses are calculated at different positions of the beamline. According to Table 2, only those dominant jitter sources (highlighted in yellow or light gold) are taken into account here. Figure 2 shows the jitter evolution of relative mean energy, RMS energy spread, bunch arrival

time and RMS bunch length for different dominant jitter sources. Note here that we only show the jitter evolution in the *Elegant*, which means it starts from the L1-output. The compressor chicane is located from s=19.4m to s=22.4m; the L4 starts at about s=26.28mm and ends at s=39.998mm; the L5 is from s=40.56mm to s=54.28mm, shown as asparagus green bars at the bottom of Fig. 2 (a)-(d).

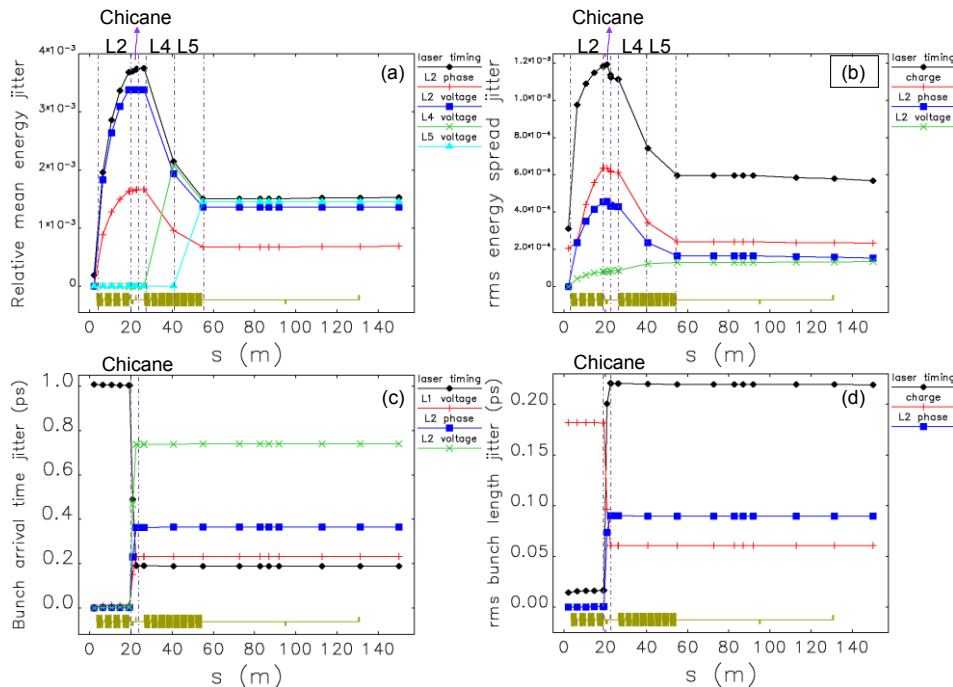


Figure 2: Beam jitter evolution for different dominant jitter sources. (a). the relative mean energy jitter evolution; (b) the RMS energy spread jitter evolution; (c) the bunch arrival time jitter; (d) the RMS bunch length jitter evolution.

Content from this work may be used under the terms of the CC BY 3.0 license (© 2018). Any distribution of this work must maintain attribution to the author(s), title of the work, publisher, and DOI.

According to Fig. 2 (a) we can see the relative mean energy ($\Delta E/E_0$) jitters that induced by laser timing, L2 phase and voltage errors grow gradually until the L4, after which the jitter decrease. This is because the mean energy(E_0) is being increased by L4 and L5. Figure 2 (b) shows that the RMS energy spread jitters due to laser timing, charge and L2 phase jitters also increase until to the L4, then goes down because of the gradually increased mean energy. The jitter caused by L2 voltage is much smaller, and only has a slight increase before L4. Figure 2 (c) shows the bunch arrival time jitter evolution for several dominant jitter sources. It is worth noting that the arrival time jitter due to the laser timing jitter is compressed by the chicane and the compression factor is about 5.6. Actually, it is demonstrated that it is possible to fully compress the arrival time jitter of the laser timing by properly adjusting the R_{56} of the chicane and keeping a moderate compression of the electron bunch [8]. On the other hand, the phase and voltage jitter of L2, the accelerator structure right before chicane, will be fully converted into the timing jitter downstream as shown in Fig. 2 (c). Figure 2 (d) displays the bunch length jitter evolution for different jitter sources. The bunch length compression of the chicane is realized by introducing an energy chirp via phasing the beam ahead of the crest in L2, thus the compress factor is sensitive to the L2 phase variations. The injector laser timing jitter is also acting like the jitter of L2 phase. Therefore, the L2 phase and laser timing jitter are the dominant jitter sources for the bunch length jitter. Figure 2 (d) shows that the bunch length jitter due to the laser timing and L2 phase suddenly increases in the chicane, but that due to the charge fluctuation drops from 0.18 ps to about 0.06 ps after the chicane. Overall, the chicane is a turning point for most of the beam jitters.

Jitter Correlations at the LEA DUT

Correlation analysis can explain the causes of the beam jitters and help us to focus efforts to optimize the design. From Table 2 in section 3.1, we roughly know that the most dominant jitter sources to the key beam parameters are laser timing, L2 phase and voltage jitters. To obtain a further insight of the correlation between the jitter sources and beam properties, we calculate the corresponding Pearson correlation coefficient C_{xy} :

$$C_{xy} = \frac{cov(x,y)}{\sigma_x \sigma_y}$$

where x and y represent a jitter source and a beam parameter jitter respectively, $cov(x,y)$ is the covariance of the two variables and σ_x, σ_y are the standard deviations of the two variables. "Responsibility" can be defined as the correlation coefficient squared C_{xy}^2 , which gives the proportion of the source error in the beam jitter.

Figure 3 shows the responsibility of all the studied jitter sources for the key beam parameters including relative mean energy, RMS energy spread, bunch arrival time and RMS bunch length. It is shown clearly that the laser tim-

ing error is strongly correlated with both the bunch length and RMS energy spread. L2 phase and voltage jitters take more responsibility for the bunch arrival time and relative mean energy jitter, in which the L2 voltage jitter even has a responsibility of more than 60% for the bunch arrival time jitter. Besides, L5 voltage jitter is also a main cause of the relative mean energy jitter. The laser timing, L2 phase and voltage jitters are the most serious sources to the beam jitters at the DUT as concluded in the above sections. Figure 4 displays the scatter plot of the beam properties and the corresponding jitter sources showing strong correlations of the 151 random seeds. The a, b, c, d correspond to the circled point in Fig. 3 respectively.

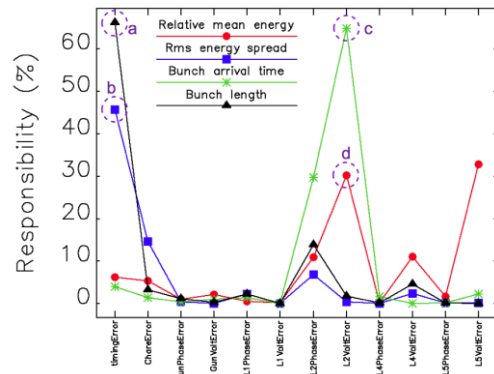


Figure 3: Responsibility of the jitter sources for the key beam parameters jitters.

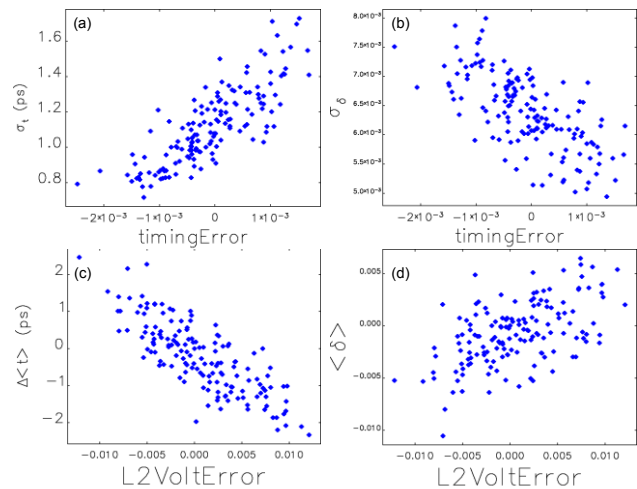


Figure 4: Scatter plots of the beam properties and the jitter sources for the 151 random seeds; (a). jitter correlation between laser timing error and bunch length; (b). jitter correlation between laser timing error and RMS energy spread; (c). jitter correlation between L2 voltage error and bunch arrival time; (d). jitter correlation between L2 voltage error and relative mean energy.

CONCLUSION

In this paper, a start-to-end jitter simulation for the APS Linac is studied on the combined use of *Astra* and *Elegant* codes taking the space charge, Schottky effect, CSR and wakefields into consideration. Beam responses at the

DUT to the jitter sources, beam jitter development along the beamline and jitter correlations at the DUT are investigated in detail. Jitter analysis reveals that the main origins of the beam jitter are the laser timing and Linac voltage jitter. In particular, requirements on laser timing, and the phase and voltage stability of the accelerator structure right before chicane are very stringent. It is worth pointing out that the arrival time jitter due to the laser timing jitter can be compressed by the the magnetic chicane by a factor of 5.6. On the other hand, the most serious beam jitters for the experiments in the DUT are the mean energy jitter which is mainly caused by voltage jitter of the accelerator structures, and bunch arrival time jitter which is mostly caused by phase and voltage jitter of the accelerator structure right after the chicane. In the future work, the effect of beam jitters on the FEL performance will be evaluated.

ACKNOWLEDGEMENTS

The authors would like to thank A. Zholents for providing helpful information and the many useful discussions. This research was supported by the U.S. Department of Energy, Office of Science, under Contract No. DE-AC02-06CH11357. The authors gratefully acknowledge financial support from University of Chinese Academy of Sciences (UCAS) for studying abroad.

REFERENCES

- [1] Y. Park *et al.*, in *Proc. 38th Int. Free Electron Laser Conf. (FEL'17)*, Santa Fe, NM, USA, Aug. 2017, pp.49-52, doi:10.18429/JACoW-FEL2017-MOP011
- [2] J. Duris, A. Murokh, and P. Musumeci, "Tapering enhanced stimulated superradiant amplification", *New. J. Phys.*, vol. 17, no. 6, p. 063036, 2015, doi:10.1088/1367-2630/17/6/063036
- [3] A. Zholents *et al.*, "A preliminary design of the collinear dielectric wakefield accelerator", *Nucl. Instrum. Methods Phys. Res. A*, vol. 829, p. 190, 2016, doi:10.1016/j.nima.2016.02.003
- [4] *ASTRA Manual*, K. Floettmann, Mar. 2017, pp. 56-64, http://www.desy.de/~mpyflo/Astra_manual/Astra-Manual_V3.2.pdf
- [5] *Elegant: A flexible SDDS-compliant code for accelerator simulation*, M. Borland, 2000, https://www.aps.anl.gov/files/APS-sync/lsn-otes/files/APS_14182K18.pdf
- [6] M. Borland, "Design and performance simulations of the bunch compressor for the Advanced Photon Source Low-Energy Undulator Test Line free-electron laser", *Phys. Rev. ST Accel. Beams*, vol. 4, no. 7, p. 074201, 2001, doi:10.1103/PhysRevSTAB.4.074201
- [7] S. Shin, Y. Sun, and A. Zholents, "Interleaving lattice for the Argonne Advanced Photon Source linac", *Phys. Rev. Accel. Beams*, vol. 21, no. 6, p. 060101, 2016, doi:10.1103/PhysRevAccelBeams.21.060101
- [8] B. Marchetti, R. Assmann, U. Dorda, J. Zhu, "Conceptual and Technical Design Aspects of Accelerators for External Injection in LWFA", *Applied Sciences*, vol. 8, no. 5, p. 757, 2018, doi:10.3390/app8050757